Bioorganic & Medicinal Chemistry Letters 19 (2009) 3177–3182

Contents lists available at ScienceDirect

Bioorganic & Medicinal Chemistry Letters

journal homepage: www.elsevier.com/locate/bmcl

Differences in CYP3A4 catalyzed bioactivation of 5-aminooxindole and 5-aminobenzsultam scaffolds in proline-rich tyrosine kinase 2 (PYK2) inhibitors: Retrospective analysis by CYP3A4 molecular docking, quantum chemical calculations and glutathione adduct detection using linear ion trap/orbitrap mass spectrometry

Hao Sun, Raman Sharma, Jonathan Bauman, Daniel P. Walker, Gary E. Aspnes, Michael P. Zawistoski, Amit S. Kalgutkar *

Pfizer Global Research and Development, Eastern Point Road, Groton, CT 06340, USA

ARTICLE INFO

Article history:
Received 13 March 2009
Accepted 24 April 2009
Available online 3 May 2009

Keywords:
P450
Reactive metabolite
Oxidation
Crystal structure
Glutathione
Orbitrap
Mass spectrometry

ABSTRACT

Previous studies have demonstrated the CYP3A4 mediated oxidation of the 5-aminooxindole motif, present in the trifluoromethylpyrimidine class of PYK-2 inhibitors, to a reactive bis-imine species, which can be trapped with glutathione (GSH) in human liver microsomal incubations. The corresponding 5-aminobenzsultam derivatives, which should possess a similar oxidative liability, do not form GSH conjugates in microsomal incubations. In the current study, we conducted a retrospective analysis on representative 5-aminooxindole and 5-aminobenzsultam PYK-2 inhibitors utilizing CYP3A4 molecular docking and quantum chemical calculations to rationalize the bioactivation differences. Our analysis revealed key differences in (a) active site binding and (b) two-electron oxidation rates, which correlate with GSH adduct formation with the two moieties. The value of linear ion/orbitrap mass spectrometry to detect GSH conjugates with greater sensitivity, compared with conventional triple quadrupole mass spectrometry approaches, was also demonstrated in the course of these studies.

Because it is now widely appreciated that reactive metabolites (RMs), as opposed to the parent molecules from which they are derived, are responsible for the pathogenesis of certain adverse drug reactions, RM formation with new chemical entities (NCEs) is generally considered a liability in the drug discovery process.[1,2] Procedures have been implemented to monitor RM formation in discovery with the ultimate goal of eliminating or minimizing the liability via rational structural modification. An example of such a situation was evident in our recent studies on the trifluoromethylpyrimidine class of proline-rich tyrosine kinase 2 (PYK2) inhibitors for the treatment of osteoporosis.[3]

Virtually, all of the trifluoromethylpyrimidine derivatives, which contained the C2 5-aminooxindole motif (exemplified with **1**) were positive in the high-throughput screen (HTS) for RM formation. This screen examines the bioactivation potential of NCEs in NADPH-supplemented human liver microsomes (HLM) via the detection of glutathione (GSH) and/or glutathione ethyl ester (GSH-EE) captured reactive intermediates.[4] Elucidation of the GSH conjugate structure of **1** provided an insight into the RM structure, which led to the proposed bioactivation pathway involving cytochrome P450 (CYP)-catalyzed two-electron oxidation of the 5-aminooxindole motif to an electrophilic bis-imine (Scheme 1).[3]

Standard medicinal chemistry tactics involving disruption of the 5-aminooxindole scaffold via replacement of the fused lactam ring with electron-withdrawing groups or reversing the carbonyl and amino groups within the lactam ring were employed to eliminate the RM liability of **1**.[3] This exercise generated several compounds, which were devoid of RM formation, while retaining the primary pharmacology and pharmacokinetic attributes associated with the 5-aminooxindole counterparts (see Scheme 1).

While it was reasonable to anticipate the absence of RM formation in cases where the electron-rich bis-aniline architecture was disrupted, we were surprised to find that the 5-aminobenzsultam derivatives (exemplified by **2**), were also devoid of the bioactivation liability (inferred from the lack of sulfydryl conjugate formation in the HTS RM screen). In theory, 5-aminobenzsultams should also form the electrophilic bis-imine via the bioactivation pathway discerned with 5-aminooxindoles (Scheme 1).

In the current studies, we utilized CYP molecular docking and ab initio quantum chemical calculations to probe differences in active site binding and two-electron oxidation rates of the 5-aminooxindole and the 5-aminobenzsultam derivatives **1** and **2**,

* Corresponding author.
E-mail address: amit.kalgutkar@pfizer.com (A.S. Kalgutkar).

0960-894X/$ - see front matter © 2009 Elsevier Ltd. All rights reserved.
doi:10.1016/j.bmcl.2009.04.118

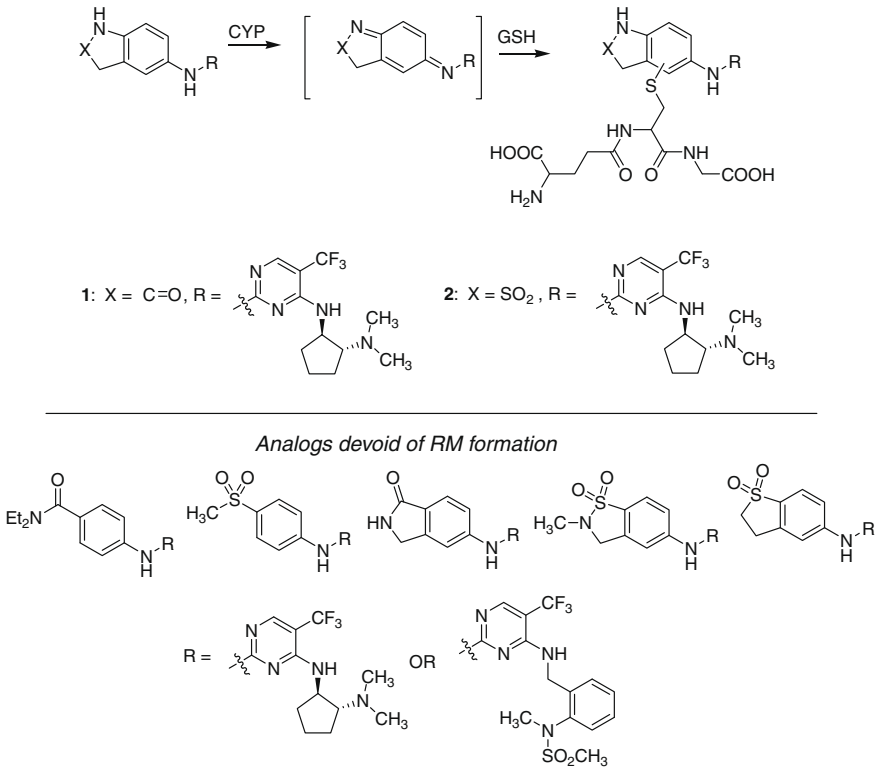

Scheme 1. Proposed mechanism of CYP-catalyzed bioactivation of 5-aminooxindole and 5-aminobenzsultam derivatives **1** and **2**, respectively.

respectively, in an attempt to provide plausible explanation(s) for the bioactivation differences. In addition, the possibility that conventional triple quadrupole mass spectrometry (MS) detection was not sensitive enough to detect GSH adducts of **2** was probed using the sensitive linear ion trap/orbitrap MS detection. The collective findings are summarized, herein.

The likelihood that greater metabolic resistance of **2** (compared with **1**) in HLM eliminates RM formation was ruled out since both compounds possess similar half-lives in HLM.[3] Next, the possibility that lack of RM formation with **2** is due to the existence of a competing and perhaps more facile metabolic pathway(s) was explored in metabolite identification studies on the two compounds. As shown in Figure 1, incubation of **1** or **2** in HLM indicated the NADPH-dependent formation of a single metabolite in both cases. The molecular weights of the metabolites were 14 mass units lower than those of the parent compounds (**1**: $MH^+ = 421$; **2**: $MH^+ = 457$) indicative of N-demethylation on the *N*,*N*-dimethylcyclopentane ring. *These studies established that **1** and **2** were subject to identical routes of metabolism in HLM*. Furthermore, the observation that the specific CYP3A4 inhibitor ketoconazole completely abolished the metabolism of **1** and **2** in HLM (data not shown) suggested a principle role for this isozyme in the overall oxidative metabolism of the two compounds.

The availability of the crystal structures of major human CYP isozymes[5–8] has facilitated molecular docking studies with substrates to predict metabolic outcomes in a retrospective fashion. Several examples have appeared in the literature, which demonstrate the value of predicting drug metabolism using molecular docking methods.[9,10] In the present situation, the binding poses of 5-aminooxindole **1** and 5-aminobenzsultam **2** in the active site of CYP3A4 were compared using the flexible molecular docking and molecular dynamics approach.[11] The analysis was restricted to CYP3A4 because of our past work, which demonstrated the exclusive involvement of this isozyme in the bioactivation of the 5-aminooxindole motif in trifluoromethylpyrimidines.[3]

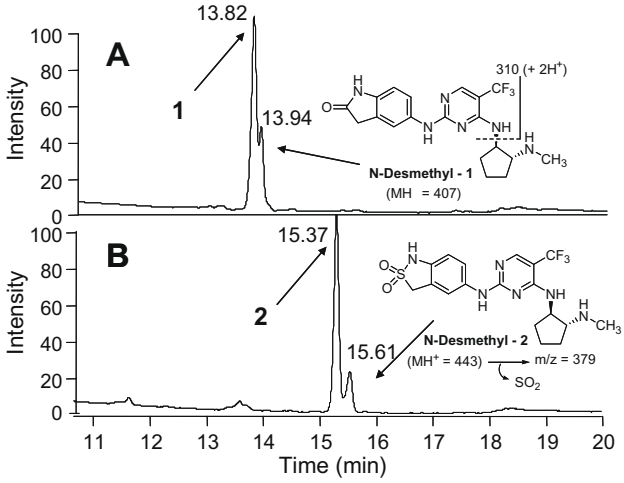

Figure 1. Photo diode array trace ($\lambda = 315$ nm) of an incubation mixture comprising of **1** (panel A) and **2** (panel B) at a concentration of 10 μM each in NADPH-supplemented HLM for 30 min. The origins of the diagnostic ions for the N-demethylated metabolites are shown and were obtained by collision-induced dissociation (CID) of the MH^+ for the metabolites. The fragment ion (*m*/*z*) at 310 in the CID spectrum of the *N*-desmethyl-**1** was also observed in the CID spectrum of the parent compound. Likewise, the fragment ion (*m*/*z*) at 379 in the CID spectrum of *N*-desmethyl-**2**, which corresponded with the loss of sulfur dioxide, changed to *m*/*z* 393 in the CID spectrum of **2**.

Figure 2 illustrates the energetically favored docking modes for compounds **1** and **2**. Both oxindole and benzsultam rings are in close proximity to the heme iron, which suggests that metabolism to the reactive bis-imine is possible in both cases. However, it is interesting to note that **1** binds closer (~3.0 Å) to the heme iron than **2** (~4.0 Å), indicating that **1** (and possibly all 5-aminooxindole-based PYK2 inhibitors) are juxtaposed at a spatially more

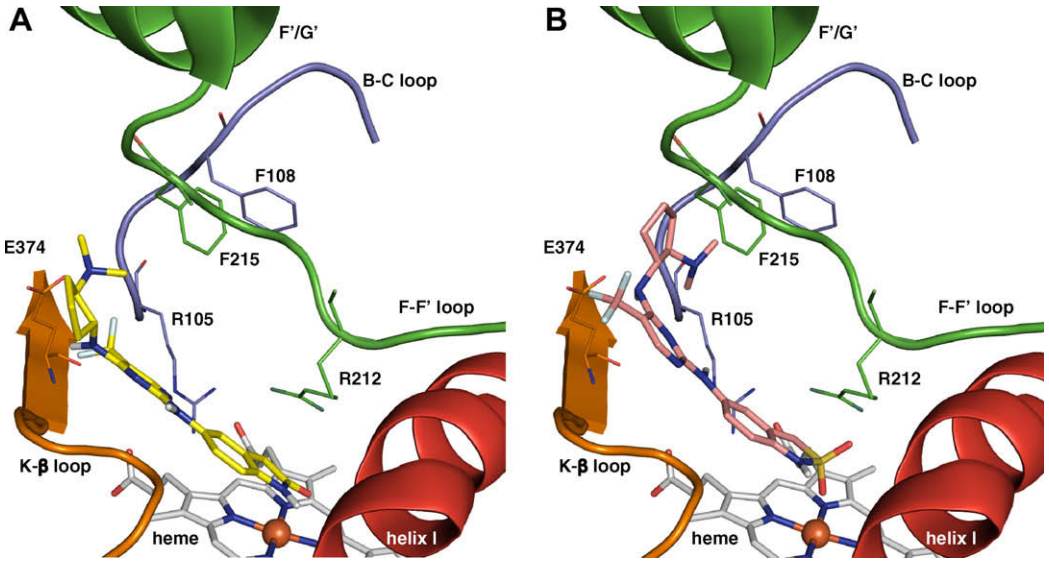

Figure 2. The binding poses of compounds **1** (A) and **2** (B) in the active site of CYP3A4 are predicted by docking. Conformations and orientations generated by autodock are clustered at RMSD = 2.0 Å according to their docking energies. The lowest energy docking clusters of both compounds are illustrated above using pymol. The distance between compound **1** and heme iron is measured ~3.0 Å, but increases to ~4.0 Å for compound **2**. CYP3A4 is shown in animated format with helices and loops in different colors and important active site residues in sticks. Compounds **1** (yellow) and **2** (pink) are shown in color-coded sticks: nitrogen = blue, oxygen = red, fluorine = cyan, and sulfur = gold.

favored position for the initial oxygenation by heme compound I,[12] and thus are more prone to RM formation than 5-aminobenzsultam-based PYK2 inhibitors. The docking modes for **1** and **2** also reveal that the sulfonyl group in **2** occupies more space above the heme iron and thus pushes the indole ring outward, which then results in movement of the *N*,*N*-dimethylcyclopentyl motif further into the active site access region comprised of the B–C and F–G loops. The calculated binding energies for both poses are very similar (~−7.5 kcal/mol), so energetically there is no difference between them. However, when comparing another binding orientation (data not shown) that shows the *N*,*N*-dimethylcyclopentyl motif closest to the heme iron, which accounts for the major pathway of metabolism (N-demethylation) in **1** and **2**, we found that the binding mode of **2** was more energetically favored. The latter observation also suggests that the two-electron oxidation of the 5-aminobenzsultam motif is less favorable when compared with the corresponding oxidation of the 5-aminooxindole group.

While affinity of **1** and **2** towards nonspecific CYP3A4 binding can be ruled out on the basis of comparable lipophilicity estimates (**1**: cLog *P*~1.76; **2**: cLog *P*~1.61) for the two compounds, there are several important active site residues in CYP3A4, which can contribute to the specific binding of **1** and **2**, thereby affecting the course of metabolism/bioactivation. For instance, the nitrogen atoms of the Arg212 guanidinium moiety in F–F′ loop of CYP3A4 are within hydrogen bonding distance to the sulfonyl group in **2** but not to the carbonyl group in **1**; such a potential H bonding interaction can pull the sulfonyl group from heme iron attenuating the bioactivation process. In addition, active site residues Phe108 and Arg105 in B–C loop, Phe215 in F–F′ loop, together with Glu374 in β-sheet 1 show more favored interaction with benzsultam moiety relative to the oxindole ring and thus juxtaposes the *N*,*N*-dimethylcyclopentane group in proximity of the heme iron for N-demethylation.

Overall, the results from the CYP3A4 molecular docking suggest a lower propensity of **2** (vs **1**) to undergo RM formation, a hypothesis, which was also predicted from ab initio reactivity calculations on the two compounds. Theoretical quantum chemical calculations have proven valuable in unraveling the ease with which certain electron-rich aromatic systems (e.g., catechols, hydroquinones, *para*-hydroxyacetanilides, etc.) undergo enzyme-catalyzed two-electron oxidations to RMs. This approach has seen some success in the retrospective ab initio analysis of acetaminophen oxidation,[13,14] and more recently, of the atypical neuroleptic drug remoxipride.[15] The activation energies of the rate-limiting first electron oxidation from indole ring of both compounds were calculated by density functional theory (DFT)/B3LYP (Becke three-parameter Lee–Yang–Parr) method using the 6-31G* basis set[16] (Table 1). Their corresponding fragments A and B were analyzed for the purpose of simplicity. Based on the calculated pK_a values of 13.67 and 9.26 for **1** and **2**, respectively, both compounds should be in the neutral state at the physiological condition (pH 7.4). Our calculation showed that 5-aminobenzsultam fragment is more difficult to oxidize with approximately +4.5 kcal/mol more energy required for oxidation. This value is within comparable range of our previous ab initio studies comparing the propensity of 4-hydroxyphenyl- and 4-hydroxypyrimidinyl-piperazine analogs to undergo two-electron oxidation to the corresponding reactive quinone-imine species. In the latter situation, an oxidation obstacle of 13.4 kcal/mol in protonated state or around 6.7 kcal/mol in neutral state virtually eliminated reactive quinone-imine formation with the 4-hydroxypyrimidinyl piperazine.[17] Ideally, a combination of quantum mechanical and molecular mechanical (QM/MM)

Table 1
Calculated energies[a] for the first electron withdrawing from the indole rings of fragments[b] A and B, using DFT B3LYP/6-31G* method

Fragments	Δ*E* (kcal/mol)	ΔΔ*E* (kcal/mol)
A	148.9	4.5
B	153.4	

[a] Absolute energies are −533.72076 hartree for A and −968.93757 hartree for B.
[b] The pK_a value is 13.67 for **1** and 9.26 for **2** as calculated by ACD/pK_a dB, therefore, the neutral fragments A and B were chosen for calculation

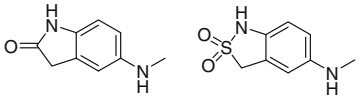

methods would predict the metabolism more precisely,[12] however, we feel that our current two-step computing methodology utilizing both molecular docking and density functional theory provided meaningful information for rationalizing bioactivation differences in **1** and **2**.

Although our in silico analyses suggested a *lower* propensity for the 5-aminobenzsultam motif in **2** to undergo two-electron oxidation to a RM (when compared with the 5-aminooxindole group in **1**), the results did not provide unambiguous data to suggest that **2** would be completely free of RM formation. Consequently, the in silico predictions contrasted somewhat with our previous HTS experimental observations on **2**, which revealed a *complete absence* of GSH-EE conjugation formation (and therefore RM formation) with the compound.[3]

A plausible explanation for this discrepancy could be that the conventional triple quadrupole MS detection technique employed in the HTS RM assay was not sensitive enough to detect low levels of RM formed in HLM incubations of **2**. Consequently, we revisited RM trapping studies on **1** and **2** in HLM using the sensitive combination of linear ion trap/orbitrap MS method for detection.[18,19] The combination of orbitrap technology with a linear ion trap is known to enable fast, sensitive and reliable detection and identification of small molecules regardless of relative ion abundance.[20]

Figures 3 and 4 depict the linear ion trap/orbitrap MS qualitative analysis[21] of NADPH- and GSH-supplemented HLM incubations containing **1** and **2**, respectively. *Sulfydryl conjugates with molecular ions (MH^+) at 726 and 762 were detected for both **1** and **2**, respectively, in a NADPH-dependent fashion*, a finding that contrasted with the results of the HTS RM assay for **2**. Inclusion of the specific CYP3A4 inhibitor ketoconazole in the HLM incubations eliminated GSH conjugate formation implicating that CYP3A4 was responsible for the oxidative metabolism as well as bioactivation of both compounds. Furthermore, additional chromatographic separation revealed the presence of two isomeric GSH adduct peaks for both **1** and **2** (Figs. 3 and 4, panel A). The molecular masses of the conjugates were consistent with the addition of one molecule of GSH to the molecular mass of the parent compounds.

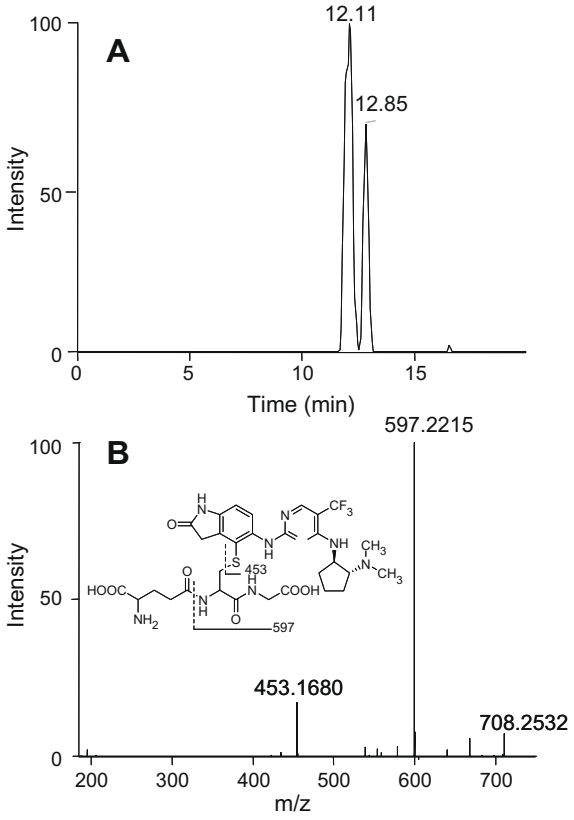

Figure 3. Extracted ion chromatogram of the GSH conjugate of **1** (10 μM) (panel A) following incubation with HLM, NADPH and GSH (5 mM). Panel B shows the product ion spectra obtained by CID of the MH^+ ion (*m/z* 726). The origins of the diagnostic ions are as indicated. The two peaks are regioisomers with identical CID patterns. MS analysis was conducted in the positive ion mode.

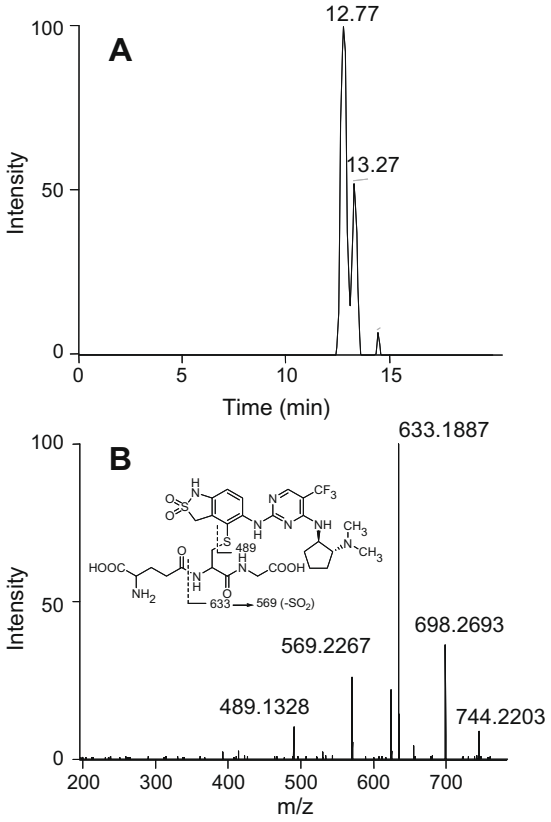

Figure 4. Extracted ion chromatogram of the GSH conjugate of **2** (10 μM) (panel A) following incubation with HLM, NADPH and GSH (5 mM). Panel B shows the product ion spectra obtained by CID of the MH^+ ion (*m/z* 762). The origins of the diagnostic ions are as indicated. The two peaks are regioisomers with identical CID patterns. MS analysis was conducted in the positive ion mode.

The CID spectra of the isomeric GSH conjugates for **1** (retention time = 12.11/12.85 min) and **2** (retention time = 12.77/13.27 min) (Figs. 3 and 4, panel B) are consistent with GSH attachment on the 5-aminooxindole and 5-aminobenzsultam groups, respectively, in these compounds.[22] The assigned regiochemistry of GSH addition as shown is arbitrary and for illustrative purposes only. Overall, the findings on GSH conjugate formation with **1** (and **2**) are consistent with those observed in our previous studies with close-in 5-aminooxindole analogs and reflect the prototypic two-electron oxidation pathway leading to the electrophilic bis-imine.[3]

Having ascertained that **2** was indeed capable of forming a GSH conjugate in a manner similar to that discerned with **1**, we next embarked on a semi-quantitative assessment of GSH adduct levels for **1** and **2** using both the linear ion trap/orbitrap and triple quadrupole MS for comparison (Fig. 5). HLM incubations with **1** and **2** were conducted at four different concentrations (1.0, 5.0. 10, and 20 μM).

Comparison of the peak area intensity of the GSH adduct of **1** and **2** on the orbitrap shows a diminished yield of the GSH conjugate of **2** (Fig. 5, panel A). This finding is consistent with the in silico predictions on the lower propensity of **2** to form RMs. The

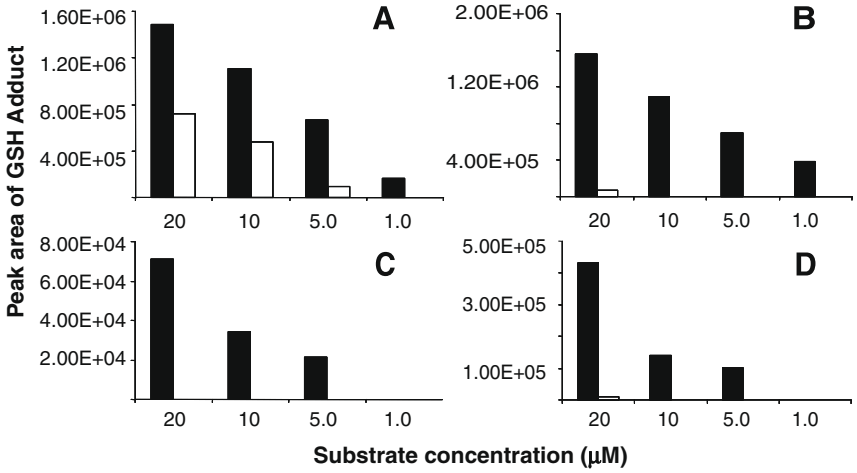

Figure 5. Peak area intensities for GSH conjugate of **1** (filled bars) and **2** (open bars) as function of substrate concentration. Panel A: Detection by linear ion trap/orbitrap MS operating in the full scan positive ion mode, Panel B: Detection by conventional triple quadrupole MS operating in a full scan positive ion mode, Panel C: Detection by conventional triple quadrupole MS operating in the negative ion mode by scanning for the precursors of *m/z*–H^+ at 272 Da, Panel D: Detection by conventional triple quadrupole MS operating in the positive ion mode and scanning for the constant neutral loss of 129 Da. Peak area intensities of the GSH conjugates are a mean of three individual microsomal incubations.

concentration-dependent increases in the GSH conjugate for both compounds appear to be a function of their relative affinity (K_m) to undergo CYP3A4 mediated oxidation to bis-imine. If so, then it is clear that **1** possesses higher affinity (lower K_m) than **2** for CYP3A4. Also of great interest are the results in panel B, wherein the triple quadrupole MS is unable to detect the GSH conjugate of **2** at the 1.0, 5.0 and 10 μM substrate concentration range. This finding is in excellent agreement with the negative HTS RM results obtained with **2** given that HLM incubations in HTS assay are conducted at a fixed substrate concentration (10 μM) and the GSH detection is performed using comparable triple quadrupole MS conditions.[4] Attempts to increase detection sensitivity of the triple quadrupole instrument by switching polarity to the negative ion mode and monitoring for the precursors of *m/z* 272 (corresponding to the anion of γ-glutamyl-dehydroalanyl-glycine, which is lost from GSH conjugate)[23] (panel C) or via monitoring for the constant neutral loss of 129 Da (a characteristic loss of the pyroglutamate moiety in GSH conjugates)[24] (panel D), proved unsuccessful in conjugate detection with **2**. Finally, it is interesting to note that a higher substrate concentration (20 μM), we were able to observe the GSH conjugate of **2** using triple quadrupole MS (panels B and D). However, the sensitivity of detection (as gauged from the peak area comparison) was still below par, when compared to the orbitrap.

In conclusion, the results from the CYP3A4 docking analysis provide logical active site substrate binding orientations to support the selectivity of CYP3A4 catalyzed oxidation of the 5-aminooxindole ring in **1** relative to oxidation of the 5-aminobenzsultam ring in **2**. In addition, ab initio calculations on the activation energies required for oxidation of the 5-aminooxindole and 5-aminobenzsultam rings also predicted that the latter substituent would be less prone to form the bis-imine RM. Thus, the combined use of CYP molecular docking, quantum mechanical calculations and biochemical experiments greatly facilitated our understanding on the bioactivation differences between **1** and **2**. As such, these approaches could be potentially utilized in drug discovery, in a proactive fashion to guide hit-to-lead efforts, when NCEs are plagued with RM and/or CYP inactivation issues. The detection of the GSH conjugate of **2** using orbitrap MS presents an interesting dogma in a prototypical drug discovery scenario, where information pertaining to RM formation with NCEs is usually assessed using triple quadrupole MS instrumentation. Consequently, it is worthwhile to exercise caution when interpreting negative RM data, particularly with NCEs, which contain known structural alerts.[25] Finally, it is noteworthy to point out that differences in bioactivation profile between the 5-aminooxindole and 5-aminobenzsultam motifs, may not representative of a general phenomenon, which can be extended to all compounds. For instance, the 4-amino-2-phenoxymethanesulfonanilide metabolite of the selective cyclooxygenase-2 inhibitor nimesulide has been shown to undergo two-electron oxidation to the reactive bis-imine metabolite.[26]

References and notes

1. Walgren, J. L.; Mitchell, M. D.; Thompson, D. C. *Crit. Rev. Toxicol.* **2005**, *35*, 325.
2. Kalgutkar, A. S.; Fate, G.; Didiuk, M. T.; Bauman, J. *Exp. Rev. Clin. Pharmacol.* **2008**, *1*, 515.
3. Walker, D. P.; Bi, F. C.; Kalgutkar, A. S.; Bauman, J. N.; Zhao, S. X.; Soglia, J. R.; Aspnes, G. E.; Kung, D. W.; Klug-McLeod, J.; Zawistoski, M. P.; McGlynn, M. A.; Oliver, R.; Dunn, M.; Li, J. C.; Richter, D. T.; Cooper, B. A.; Kath, J. C.; Hulford, C. A.; Autry, C. L.; Luzzio, M. J.; Ung, E. J.; Roberts, W. G.; Bonnette, P. C.; Buckbinder, L.; Mistry, A.; Griffor, M. C.; Han, S.; Guzman-Perez, A. *Bioorg. Med. Chem. Lett.* **2008**, *18*, 6071.
4. Soglia, J. R.; Harriman, S. P.; Zhao, S.; Barberia, J.; Cole, M. J.; Boyd, J. G.; Contillo, L. G. *J. Pharm. Biomed. Anal.* **2004**, *36*, 105. Glutathione ethyl ester (GSH-EE) is used as the exogenous trapping agent in the HTS RM assay due to increased sensitivity in sulfydryl conjugate detection with the ethyl ester derivative of GSH relative to the free carboxylic acid, a feature attractive for HT screening.
5. Yano, J. K.; Wester, M. R.; Schoch, G. A.; Griffin, K. J.; Stout, C. D.; Johnson, E. F. *J. Biol. Chem.* **2004**, *279*, . 38091.
6. Wester, M. R.; Yano, J. K.; Schoch, G. A.; Yang, C.; Griffin, K. J.; Stout, C. D.; Johnson, E. F. *J. Biol. Chem.* **2004**, *279*, 35630.
7. Williams, P. A.; Cosme, J.; Vinkovic, D. M.; Ward, A.; Angove, H. C.; Day, P. J.; Vonrhein, C.; Tickle, I. J.; Jhoti, H. *Science* **2004**, *305*, 683.
8. Schoch, G. A.; Yano, J. K.; Wester, M. R.; Griffin, K. J.; Stout, C. D.; Johnson, E. F. *J. Biol. Chem.* **2004**, *279*, 9497.
9. Sun, H.; Moore, C.; Dansette, P. M.; Kumar, S.; Halpert, J. R.; Yost, G. S. *Drug Metab. Dispos.* **2009**, *37*, 672.
10. Sun, H.; Yost, G. S. *Chem. Res. Toxicol.* **2008**, *21*, 374.
11. Molecular docking: The structure of compounds **1** and **2** was first built using Chem3D (CambridgeSoft Corporation, Cambridge, MA); their geometries were optimized using the molecular mechanics method (MM2) followed by the density functional theory (DFT)/B3LYP (Becke three-parameter Lee–Yang–Parr) method using the 6-31G basis set in gaussian 03 (Gaussian, Inc., Wallingford, CT). The energetically minimized structure of compounds **1** and **2** was further modified by autodocktools program (The Scripps Research Institute) with the Gasteiger atomic charges assigned and flexible torsions defined. Three-dimensional coordinates of CYP3A4 structure were acquired both from Research Collaboratory for Structural Bioinformatics Protein Data Bank [PDB code: 1TQN, 1W0E, 1W0F, 1W0G, 2J0D, and 2V0M] and Pfizer protein structure database (11 structures with various substrate bound). A modified CYP3A4 structure template based on the dynamic analysis of all templates and over 30 well-characterized CYP3A4 substrates (Pfizer compounds) was chosen for molecular docking, which was modified with polar hydrogens, Kollman partial

charges, and solvation parameters added using autodocktools. The active site space was defined using AutoGrid 4 (The Scripps Research Institute), which precalculates grids of van der Waals, hydrogen bonding, electrostatics, torsion, and solvation interactions between CYP3A4 and substrates (**1** and **2**). Autodock 4 (The Scripps Research Institute) searched the globally optimized conformations and orientations of **1** and **2** using the Lamarckian genetic algorithm, a hybrid of a genetic algorithm with an adaptive local search method. Docking was accomplished on Pfizer LSF (load sharing facility) Linux GRID. Four thousand LGA runs were conducted and followed by a cluster analysis. Docking solutions with compounds **1** and **2** all-atom root mean square deviation (RMSD) within 2.0 Å of each other were clustered together using autodocktools, and the best ranked clusters by the lowest docking energy were selected for analysis.

12. Kuhn, B.; Jacobsen, W.; Christians, U.; Benet, L. Z.; Kollman, P. A. *J. Med. Chem.* **2001**, *44*, 2027.
13. Koymans, L.; van Lenthe, J. H.; van de Straat, R.; Donné-Op den Kelder, G. M.; Vermeulen, N. P. *Chem. Res. Toxicol.* **1989**, *2*, 60.
14. Koymans, L.; Van Lenthe, J. H.; Donné-op Den Kelder, G. M.; Vermeulen, N. P. *Mol. Pharmacol.* **1990**, *37*, 452.
15. Erve, J. C.; Svensson, M. A.; von Euler-Chelpin, H.; Klasson-Wehler, E. *Chem. Res. Toxicol.* **2004**, *17*, 564.
16. *Quantum chemical calculation*: Two model 5-aminooxindole and 5-aminobenzsultam fragments (Table 1, A and B) were used to estimate possible electronic effects on the metabolic rates of compounds **1** and **2** for the formation of bis-imine RMs. All atoms which are likely to have effects on the electronic structures of reactive bis-imine intermediates are included in the selected fragments. The pK_a value was calculated as 13.67 for **1** and 9.26 for **2** by ACD/PhysChem Suite (Advanced Chemistry Development, Inc., Toronto, Ontario, Canada), so the neutral state fragments were chosen for the following ab initio calculation by gaussian 03 (Gaussian, Inc., Wallingford, CT). The electron abstraction energies from the aromatic rings were calculated by the density functional theory (DFT)/B3LYP (Becke three-parameter Lee–Yang–Parr) method with the 6-31G basis set selected. The calculation was accomplished on Pfizer PBS (portable batch system) Linux GRID in parallel.
17. Kalgutkar, A. S.; Vaz, A. D.; Lame, M. E.; Henne, K. R.; Soglia, J.; Zhao, S. X.; Abramov, Y. A.; Lombardo, F.; Collin, C.; Hendsch, Z. S.; Hop, C. E. *Drug Metab. Dispos.* **2005**, *33*, 243.
18. Peterman, S. M.; Duczak, N., Jr.; Kalgutkar, A. S.; Lame, M. E.; Soglia, J. R. *J. Am. Soc. Mass Spectrom.* **2006**, *17*, 363.
19. Ruan, Q.; Peterman, S.; Szewc, M. A.; Ma, L.; Cui, D.; Humphreys, W. G.; Zhu, M. *J. Mass. Spectrom.* **2008**, *43*, 251.
20. Hardman, M.; Makarov, A. A. *Anal. Chem.* **2003**, *75*, 1699.
21. The LC–MS system consisted of a Surveyor HPLC system, an Orbitrap mass spectrometer (Thermo Fisher Scientific, Bremen, Germany) and an HPLC column (Phenomenex, Synergy RP, 150 × 4.6 mm, 4 μm, Phenomenex, Torrance, CA). HPLC was performed at a constant flow rate of 700 μL/min using a binary solvent system: Solvent A, HPLC grade water in 0.1% formic acid and Solvent B, acetonitrile water in 0.1% formic acid. The initial HPLC gradient system was held at 5% B for 3 min and linearly increased to 50% B in 22 min, followed by a return to initial conditions for column re-equilibration. Mass spectroscopy analyses were carried out in the positive ion mode using full-scan MS with a mass range of 200–500 Da and data-dependent MS/MS acquisition on the two most intense ions using the Orbitrap. The resolving power used for this experimental method was 15,000 for the full-scan event. The resolving power for MS/MS spectral events was set at 7500 in order for the total circling time to be within approximately 2 s. Dynamic exclusion was conducted by utilizing a repeat count of one prior to exclusion. Each mass-to-charge (m/z) value identified by performing a data-dependent MS/MS experiment resided on the dynamic exclusion list for 20 s. All experimental data were acquired using external calibration prior to data acquisition.
22. The fragment ions at m/z 453 and m/z 489 in the CID spectra of the GSH conjugate of **1** and **2**, respectively, were assigned as cleavage adjacent to the cysteinyl thioether moiety with charge retention on the 5-aminooxindole and 5-aminobenzsultam residues. The occurrence of these fragment ions is consistent with the presence of an aromatic thioether motif in **1** and **2**. See Ref. 24.
23. Dieckhaus, C. M.; Fernández-Metzler, C. L.; King, R.; Krolikowski, P. H.; Baillie, T. A. *Chem. Res. Toxicol.* **2005**, *18*, 630.
24. Baillie, T. A.; Davis, M. R. *Biol. Mass. Spectrom.* **1993**, *22*, 319.
25. Kalgutkar, A. S.; Gardner, I.; Obach, R. S.; Shaffer, C. L.; Callegari, E.; Henne, K. R.; Mutlib, A. E.; Dalvie, D. K.; Lee, J. S.; Nakai, Y.; O'Donnell, J. P.; Boer, J.; Harriman, S. P. *Curr. Drug Metab.* **2005**, *6*, 161.
26. Li, F.; Chordia, M. D.; Huang, T.; Macdonald, T. L. *Chem. Res. Toxicol.* **2009**, *22*, 72.